Flight solar calibrations using the mirror attenuator mosaic (MAM): Low scattering mirror

Robert B. Lee III

Atmospheric Sciences Division
NASA Langley Research Center, Hampton, Virginia 23665-5225

ABSTRACT

Measurements of solar radiances reflected from the mirror attenuator mosaic (MAM) were used to calibrate the shortwave portions of the Earth Radiation Budget Experiment (ERBE) thermistor bolometer scanning radiometers. The MAM is basically a low scattering mirror which has been used to attenuate and reflect solar radiation into the fields of view for the broadband shortwave (0.2 to 5 micrometers) and total (0.2 to 50.0+ micrometers) ERBE scanning radiometers. The MAM assembly consists of a tightly packed array of aluminum, 0.3175-cm diameter concave spherical mirrors and field of view limiting baffles. The spherical mirrors are masked by a copper plate, electro-plated with black chrome. Perforations (0.14 centimeter in diameter) in the copper plate serve as apertures for the mirrors. Black anodized aluminum baffles limit the MAM clear field of view to 7.1 degrees. The MAM assemblies are located on the Earth Radiation Budget Satellite (ERBS) and on the National Oceanic and Atmospheric Administration NOAA-9 and NOAA-10 spacecraft.

The 1984-1985 ERBS and 1985-1986 NOAA-9 solar calibration data sets are presented. Analyses of the calibrations indicate that the MAM exhibited no detectable degradation in its reflectance properties and that the gains of the shortwave scanners did not change. The stability of the shortwave radiometers indicates that the transmission of the Suprasil W1 filters did not degrade detectably when exposed to Earth/atmosphere-reflected solar radiation.

1. INTRODUCTION

The Earth Radiation Budget Experiment (ERBE) is being used to measure diurnal variability in the components of the Earth radiation budget over the entire globe as well as over geographical regions as small as 250 kilometers[1]. The components are the incoming solar radiance, the Earth/atmosphere-reflected solar radiance, and the Earth/atmosphere-emitted radiances. The solar energy absorbed by the Earth/atmosphere system should be equal to the energy lost to space by the process of emission if the system is to be in equilibrium. If the Earth/atmosphere system absorbs more energy than it loses to space, the Earth's temperature will increase until equilibrium is reached. If the Earth/atmosphere system absorbs less energy than it loses to space, the Earth's temperature will decrease. The ERBE measurements have been used to evaluate the magnitude of cloud forcing[2] on the Earth radiation budget.

ERBE has adopted a goal of measuring the components with accuracies approaching 1%. The ERBE mission objectives and scientific goals are described by Barkstrom[3]. The ERBE instrumentation consists of three Earth-viewing, narrow field of view (FOV), scanning radiometers; four Earth-viewing, wide angle, nonscanning radiometers; and an active cavity solar monitor which are located on the NASA Earth

0-8194-0602-3/91/$4.00 SPIE Vol. 1493 Calibration of Passive Remote Observing Optical and Microwave Instrumentation (1991) / 267

Radiation Budget Satellite (ERBS) and on the National Oceanic and Atmospheric Administration NOAA-9 and NOAA-10 spacecraft. The ERBS was launched September 5, 1984, while the NOAA-9 and NOAA-10 spacecraft were launched December 12, 1984, and September 17, 1986, respectively. The ERBE radiometers were designed, built, and tested under NASA contract by TRW. The scanning radiometers are described by Kopia[4] while the nonscanning radiometers are described by Luther et al.[5] The solar monitor is described by Lee et al.[6] Calibration results for the scanning and nonscanning radiometers have been presented by Lee et al.[7] and Paden et al.[8], respectively.

In this paper, the solar calibration instrumentation and approaches for the scanning radiometers are described in considerable detail. Emphasis is placed upon evaluating the stability of the MAM solar diffusing plate. Flight and ground MAM calibration measurements are presented and compared.

2. INSTRUMENTATION

The solar calibration instrumentation for the scanning radiometers is the mirror attenuator mosaic (MAM) assembly which consists of baffles and arrays of mirrors which guide the reflected sunlight into the FOV of a radiometer. The shortwave and total scanning radiometers had MAM assemblies. In Fig. 1, the shortwave and total scanner MAM baffle ports are shown in a schematic diagram of the ERBE scanning radiometric package. The telescopes of the shortwave, longwave,

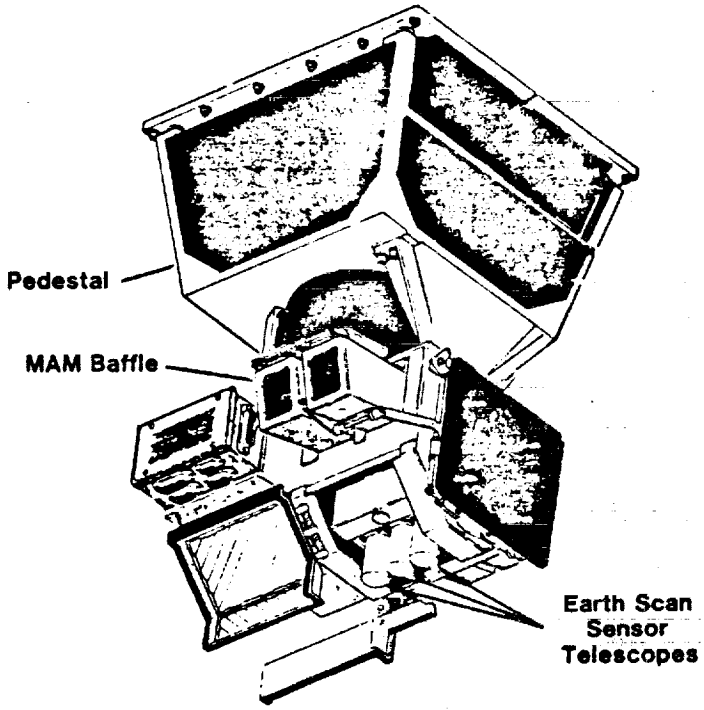

Fig. 1. Earth Radiation Budget Experiment (ERBE) scanning radiometric package.

and total scanners are shown at the bottom of the package. The longwave radiometer did not have a MAM assembly. The longwave portion of the solar spectrum, less than 0.5% of the total energy, is difficult to measure at the 1% accuracy level. The

MAM front entrance ports and baffles are designed to reject direct illumination of the MAM from either the Earth or from emitting/reflecting spacecraft components. The optical axes of the baffles are located approximately 11 degrees below any

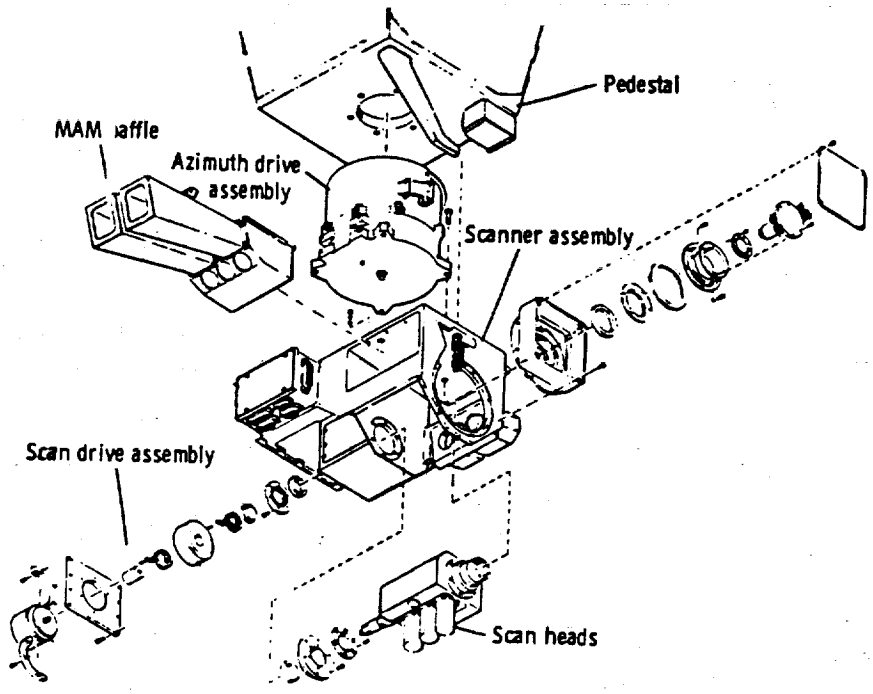

Fig. 2. Exploded diagram of the mirror attenuator mosaic (MAM) assembly.

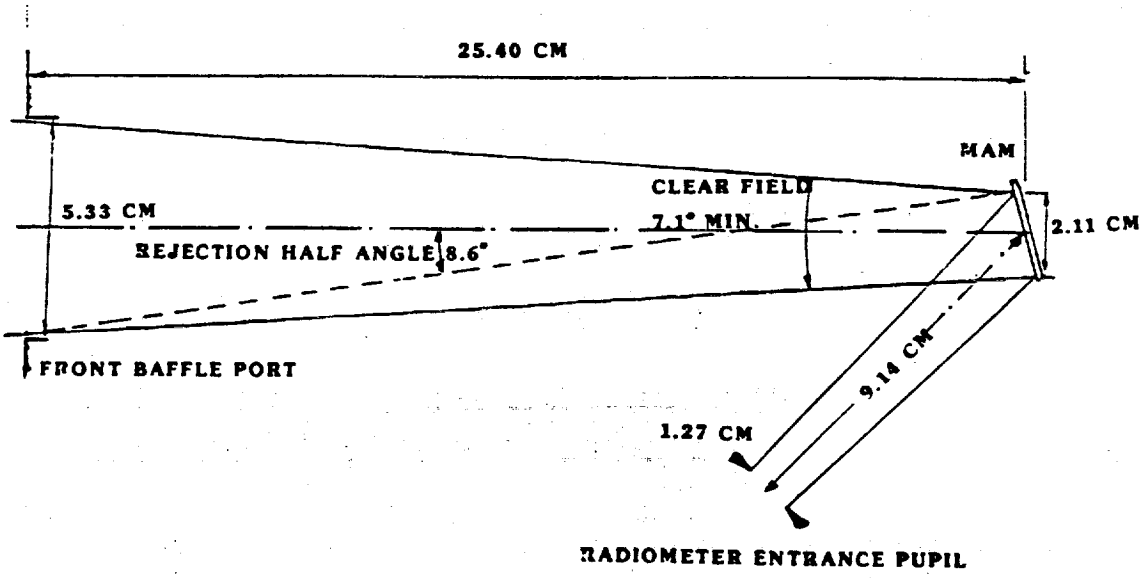

Fig. 3. Elevation view of the MAM assembly.

spacecraft structures. The minimum angle between the spacecraft structure and the Earth's horizon would be 22 degrees at the ERBS orbital altitude. Therefore, the horizon would be 11 degrees away from the optical axes. An exploded diagram of the scanning radiometric package is presented in Fig. 2. The three circular apertures in the MAM assembly permitted the scanning radiometers to view the MAM solar low scattering mirror structure. An elevation view of the MAM assembly is presented in Fig. 3. Each baffle entrance port was 5.33 centimeters (cm) in elevation height and located 25.4 cm from the MAM mirror structure. The normal to the MAM mirror structure was oriented 15 degrees below the optical axis of the baffle. The entrance pupil entrance for each radiometer was located 9.14 cm from the mirror structure. The optical axis of the radiometer was oriented 27 degrees below the normal to the mirror structure. In the elevation plane, each radiometer had an unobstructed, clear FOV of at least 7.1 degrees through the MAM ports. The ports and baffles rejected any external radiances 8.6 degrees below and above the optical axis of the baffle. The FOV of the radiometer was 4.5 degrees and the diameter of its entrance pupil was 1.27 cm.

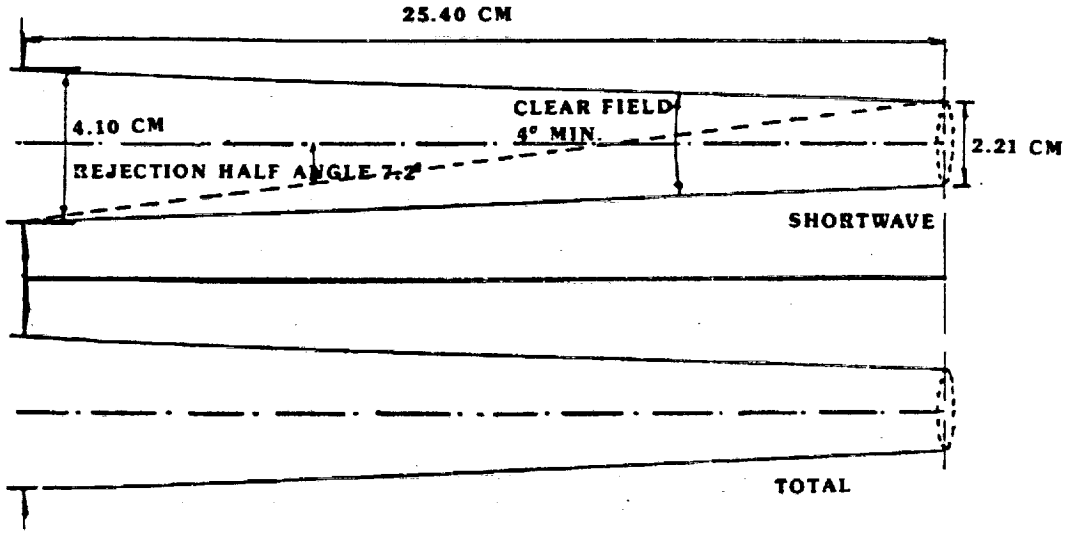

Fig. 4. Azimuthal view of the MAM assembly.

In Fig. 4, an azimuthal view of the MAM assembly shows that the MAM ports were 4.10 cm in azimuthal width. The optical axes of the shortwave and total baffles were 6.604 cm apart. In the azimuthal plane, the radiometers had clear FOV's of 4 degrees. The ports/baffles allowed only external radiances with incidence angles within $\pm$ 7.2 degrees of the baffle optical axis to be sensed by the radiometers.

The MAM mirror structure consists of an aperture mask and an array of 101 aluminum spherical mirrors. The aperture mask is made of a copper plate which is plated with a 0.0013 centimeter thick layer of nickel. Black chrome was electro-plated on the nickel layer. The thickness of the copper plate was 0.005 centimeter. The 3.175-cm by 3.175-cm mask had 0.14-cm diameter perforations which covered approximately 16% of mask area. The spherical mirrors were 0.3175 cm in diameter. The perforations served as apertures for the spherical mirrors. In Fig. 5, the geometry of a single-mirror cell is shown. The mirrors were 0.09525 centimeter deep. Incoming external radiances with the full range of incident angles between

6.4 and 23.6 degrees with respect to the mirror normal could be reflected towards the radiometer at a reflection angle of 27 degrees. The clear FOV through the baffles included incident angles between 11.4 and 18.6 degrees. The longwave radiometer sensed radiances which were emitted by the black chrome electro-plated on the copper mask with no perforations. The temperatures of MAM mirror arrays and baffles were monitored using thermistors which were embedded in each baffle and mirror array.

3. MEASUREMENTS

The ERBE scanner solar calibrations are designed to evaluate the stabilities of the shortwave scanner's gain and the shortwave portion of total scanner's gain. The

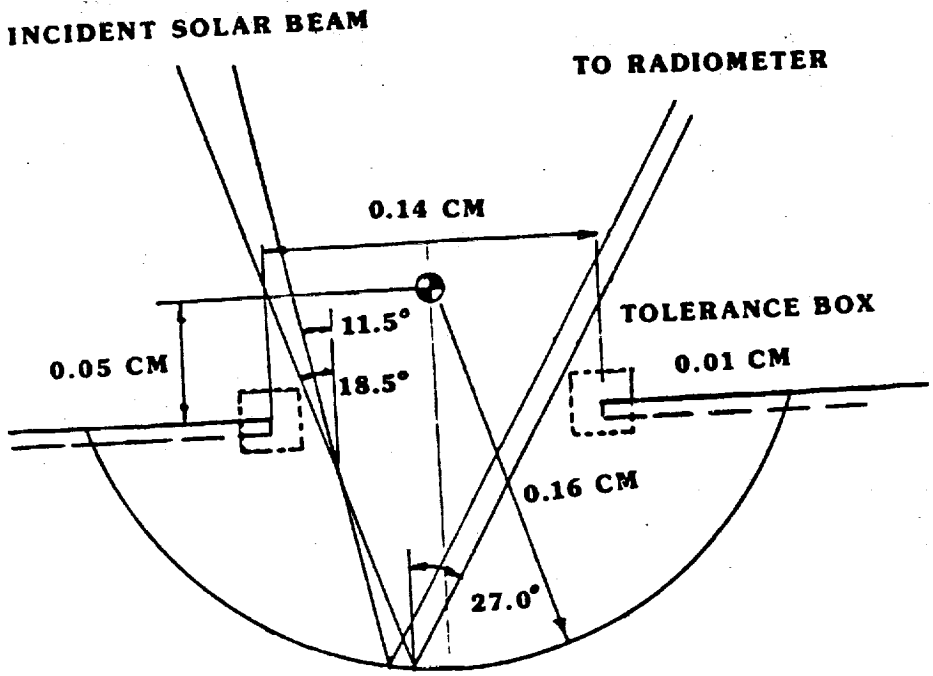

Fig. 5. Geometry of a single spherical mirror cell.

calibration sequence includes observations of space (near-zero radiance source) through the MAM both before and after the observation of the Sun. The Sun is allowed to drift through the baffle FOV and within 0.5 degrees of its optical axis. The differences in scanner output signals which are measured during the solar and space observations are used to define the magnitude of the reflected solar radiance.

In Fig. 6, the geometry of the solar calibration measurements is illustrated. During the calibration mode, the scanners observed the MAM, the flight internal calibration module (ICM) sources, and space. The ICM sources are blackbodies for the total and longwave radiometers while the shortwave radiometer source was a tungsten lamp which was operated at four different radiance levels, including the lamp-off configuration for zero radiance. During solar calibrations, the ICM sources were not activated. Over each 4 second cycle, 74 data samples were obtained. Eight samples corresponded to reference measurements of space at an

elevation angle of 163 degrees while four samples corresponded to measurements of the radiances from the ICM sources at the elevation angle of 190 degrees. The remaining samples corresponded to observations of the MAM at the elevation angle of 233 degrees. The incoming solar radiances with incident angles within ± 8.6 degrees of the baffle optical axis were reflected by the array of MAM spherical mirror cells into the scanners' FOV's. As illustrated in Fig. 6, the baffle-optical axis was oriented 15 degrees above the MAM surface normal. During observations of the MAM, the orientation of the scanners' optical axes with respect to the MAM normal was fixed at 27 degrees. The output signals of the scanners were in volts, and the voltages were converted into the International System of measurement units using the equations which are described by Lee et al.[9] and Halyo et al.[10]. The clear FOV of the baffle was calculated to be approximately 7.1 degrees in the elevation direction.

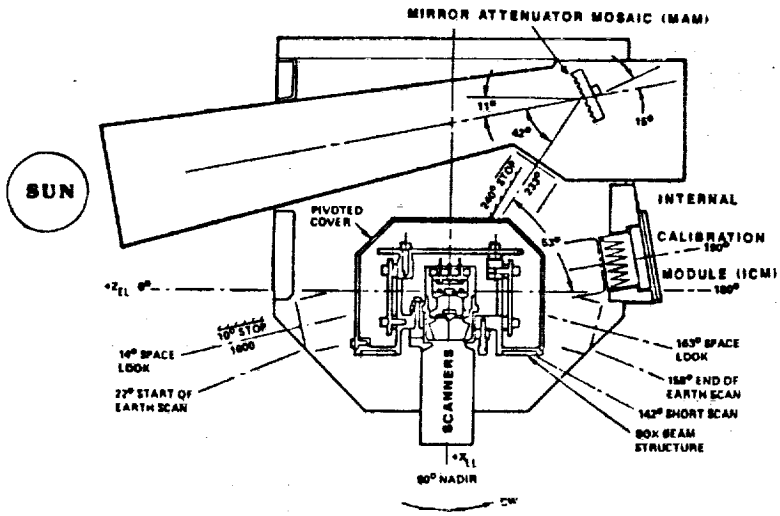

Fig. 6. Solar calibration geometry.

It was 4.0 degrees in the azimuth direction. In the elevation direction, the incident angle for the incoming solar radiances varied from 6.4 to 23.6 degrees. The angles were calculated with respect to the MAM normal. In the azimuthal direction, the incident angle varied from 15.0 to 16.6 degrees.

3.1 Ground calibration facility[12]

Using ground facilities, the MAM assemblies were evaluated to define their fields of view, the attenuation coefficients for the mirror arrays, and the quality of the scanners' gains which were derived from observations of an integrating sphere and a reference blackbody[9]. The attenuation coefficient represents the fraction of the incident shortwave radiance which is reflected by the MAM into the radiometer's FOV and is sensed by the radiometer. The MAM assemblies for the scanners were evaluated in the TRW vacuum calibration chamber[11] which are shown in Fig. 7. The chamber provided a radiometric environment which simulated the orbital conditions.

It was 2.13 meters in diameter and 2.44 meters in length. A 30.5-cm diameter, 5-kilowatt, Xenon lamp was used to simulate the radiances from the Sun. In the figure, the lamp is labeled as the solar simulator, and it was located external to the chamber. Inside the chamber, a space reference source was used to simulate the near-zero radiance of space at the elevation angle of 163 degrees. The simulated space source was a 27.9-cm diameter, grooved blackbody which was maintained at 78°K using liquid nitrogen. The ground calibration sequence included observations of the MAM, the ICM, and the simulated space source over a 4-second cycle as described in the preceding section. The scanning radiometric package was mounted to a carousel which rotated in the elevation direction. By rotating the carousel clockwise and counterclockwise, incoming radiances were sensed over an 18-degree incident angle range. The counterclockwise direction was considered to be in the negative angular-elevation direction.

The incident radiance of the Xenon lamp was defined using an electrically calibrated pyroelectric radiometer (ECPR) and a photo solar cell which were located inside the TRW vacuum calibration facility and in the incident beam. Measurements from the ECPR and solar cell established the temporal stability of the incident radiance beam at 0.9% level over a 30-minute period. The spatial uniformity of the beam was found to be 6.7% using the ECPR measurements. During the ground characterizations of the MAM assemblies, only the solar cell was used to define the magnitude of the incident radiances. Therefore, the absolute measurements of the

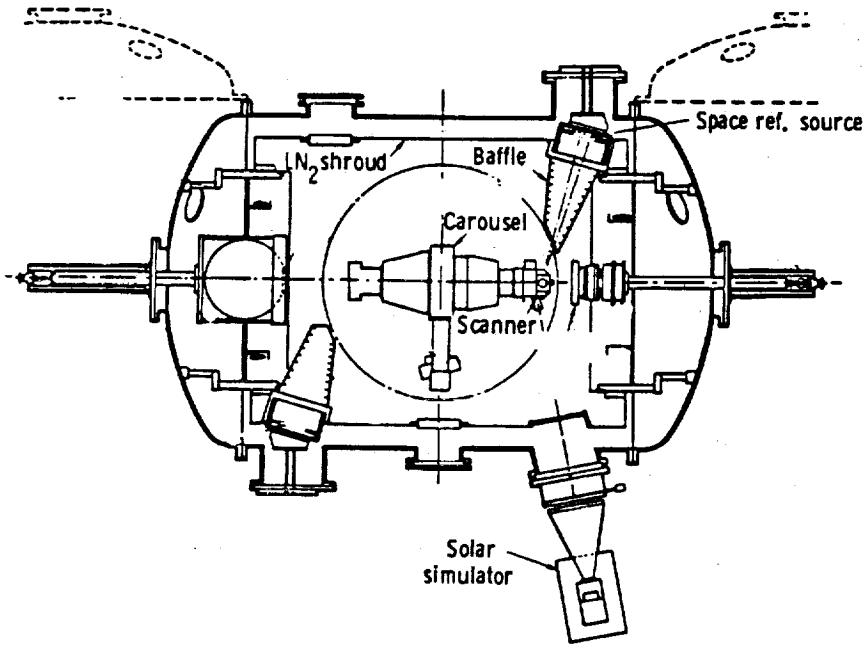

Fig. 7. ERBE vacuum calibration chamber.

ECPR had to be regressed against output voltages from the solar cell in order to calibrate and convert the cell measurements into SI units. The shortwave incident radiances, F_{sw}, were calculated using the following equation

$$F_{sw} = -4810\ (V_{sc})\ Wm^{-2}sr^{-1}mw^{-1} \qquad (1)$$

where V_{sc} is the output of the solar cell in milliwatts(mw). The angular divergence of the beam was measured and found to be less than 0.5 degree.

4. DISCUSSIONS

4.1 Ground calibration results

The solar shortwave reflected radiances should be constant[12] as the incident angle is varied between 11.4 and 18.6 degrees with respect to the normal to the MAM mirror arrays (off-axis angles of -3.6 degrees below and +3.6 degrees above the optical axes of the MAM baffles). The off-axis angle is the angle between direction to the incident radiance beam and the optical axis of the MAM baffle. This angular range represents the calculated, clear FOV interval for the MAM baffles. Therefore, the reflected solar radiances should show no detectable dependence upon the incident angle. In the ground evaluations of the MAM, the resultant measurements indicated that the magnitudes of the reflected radiances varied inversely with the incident angle of the incoming radiances. In Fig. 8, the FOV ground shortwave radiometer measurements exhibit systematic decreases in the reflected radiances of the order of 10% (ERBS and NOAA 9) to 20% (NOAA 10) over the off-axis incident angle interval between -5 to +3 degree range with respect to the baffle optical axis. This range corresponds to angles ranging from 10 to 18 degrees with respect to the MAM normal. In addition, the radiances

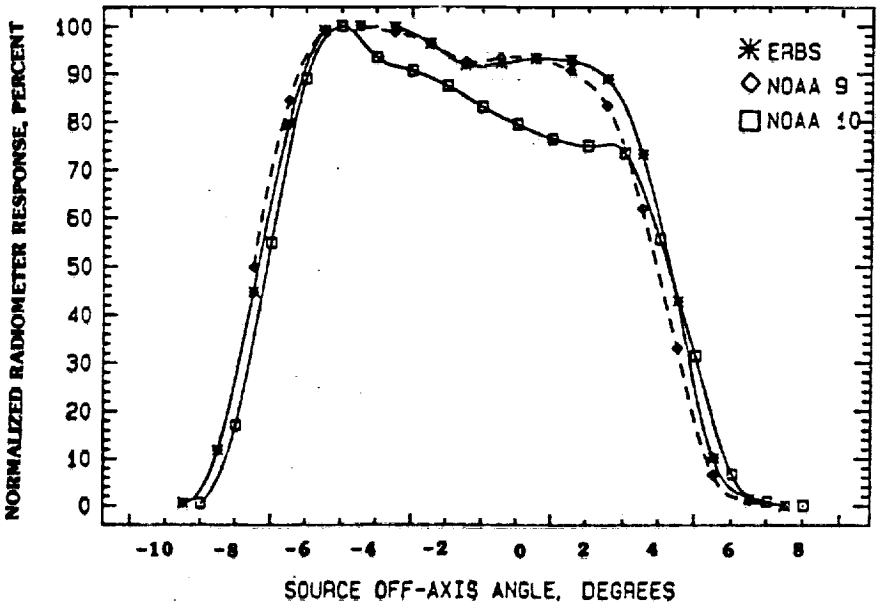

Fig. 8. Ground shortwave radiometer MAM-reflected shortwave radiances plotted against angular distance of incident beam from the optical axis of the MAM baffle.

reflected from both the ERBS and NOAA-9 shortwave MAM assemblies exhibited unexpected dips in the radiance profiles at angles approaching -1 degree, near the optical axes of the baffles. The cause of the dips is unknown. The clear FOV's (off-axis incident angle range from -5 to +3) were found to be larger than the

calculated -3.6- to +3.6-degree range. The FOV cut-off angles of -9 and +8 are in agreement with the calculated ones of -8.6 and +8.6. The NOAA-9, ERBS, and NOAA-10 FOV tests were conducted on May 6, 1983, November 20, 1983, and February 18, 1984. In addition to the FOV tests, the attenuation coefficients for the shortwave radiometer MAM's were derived. The May 6, 1983, tests of the NOAA-9 scanners indicated that the MAM for the shortwave radiometers had an attenuation coefficient of 21.05% in the direction of the radiometer. The magnitude of the incident radiance from the Xenon lamp was found to be at the 426.1 $Wm^{-2}sr^{-1}$ level, according to the solar cell measurements. The magnitude of the incident radiances was calculated using Eq. 1. The shortwave radiometer sensed 89.7 $Wm^{-2}sr^{-1}$. The November 20, 1983, tests of the ERBS scanners yielded 20.00% for the shortwave radiometer MAM attenuation coefficient. The solar cell indicated that the magnitude of the incident radiances was at the 385.5 $Wm^{-2}sr^{-1}$ level. The shortwave radiometer measured 77.1 $Wm^{-2}sr^{-1}$. The February 12, 1984, tests of the NOAA-10 scanners yielded 20.67% as the attenuation coefficient for the shortwave MAM. The solar-cell measurement yielded the magnitude of the incident radiance at the 397.7 $Wm^{-2}sr^{-1}$ level. The shortwave radiometer measured the reflected radiances from the MAM at the 82.2 $Wm^{-2}sr^{-1}$ level.

The total radiometers measured not only the shortwave radiances which were reflected from the MAM's, but also the longwave radiances which were emitted and reflected by the MAM's. Therefore, the longwave components had to be subtracted from the total measurements in order to define the MAM reflected shortwave components. For the ground measurements, the longwave components were derived from the total radiometer MAM observations with the shortwave source absence from the MAM FOV.

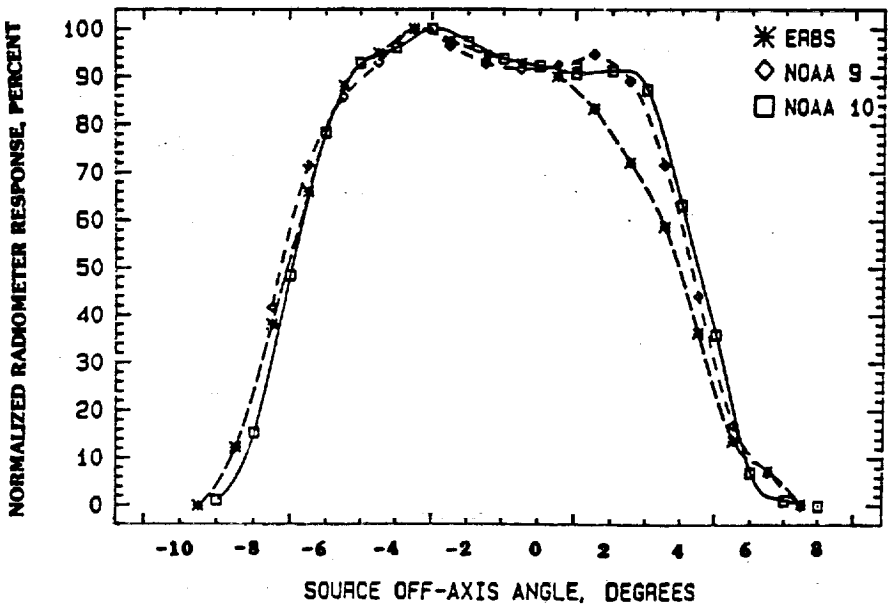

Fig. 9. Ground total radiometer MAM-reflected shortwave radiances plotted against angular distance of incident beam from the optical axis of the MAM baffle.

In Fig. 9, the total radiometer FOV measurements are presented for the same days as those for the shortwave radiometers measurements. Similar to the shortwave radiometer results, the total radiometers measurements indicated that the magnitudes of the shortwave reflected radiances varied with the off-axis incident angle. The ERBS measurements did not exhibit the dip in the reflected radiance profile which was observed in the shortwave data. The absence of the ERBS dip might have been caused by the use of a constant longwave component which might have been varying during the periods when the shortwave source was in the MAM FOV. The total NOAA-10 measurements exhibited a dip which was not present in the shortwave measurements. The measured, clear FOV's were found to be larger than the calculated ones and to lie between -5 and +3 degrees as in the cases of the shortwave radiometer MAM's. In Fig. 9, the cut-off FOV angles were found to be -9 and +8 degrees, similar to the cases of the shortwave radiometer FOV measurements.

4.2 Flight solar calibrations

Scanner solar calibrations were conducted once every 14 days during a single orbital revolution on a Wednesday. The ERBS calibrations were conducted during the November 20, 1984, through October 16, 1985, period while the NOAA-9 calibrations were conducted for a longer period of time from February 20, 1985, through December 24, 1986. The NOAA-10 calibration was limited to a single observation which occurred on November 12, 1986. The NOAA-9 calibrations were limited to a 2-year period because the scanning mechanism failed[13] on January 21, 1987. The ERBS and NOAA-10 solar calibrations were discontinued in order to prevent the scanning mechanisms from failing in the solar calibration mode[13]. The NOAA-10 and ERBS scanning radiometers failed May 1989 and February 1990, respectively.

The scanner automated solar calibration sequence[4] was divided into three measurement periods. Each period was slightly less than 7 minutes in duration. In each of the periods, the radiometers observed the MAM mirrors, space, and the ICM during each 4-second scan cycle as described Section 3. In the first period, the radiometers observed space (near-zero radiance source) through the MAM at an azimuthal "A" position where the Sun could not drift into the MAM baffle FOV's and where the Sun could not be observed directly by the radiometers at the reference space position, elevation angle of 163 degrees. In the second period, the radiometers were rotated to an azimuthal position "B" where the Sun could drift through the baffle FOV's and its radiances could be reflected by the MAM mirrors into the radiometers' FOV's. In the final period, the radiometers were rotated back to azimuthal position "A" where near-zero radiances from space could be observed in the solar-calibration scan mode.

The off-axis incident angles were calculated from the ephemerides of the Sun and spacecraft and from the alignments of the MAM baffle axes with respect to the spacecraft axes. The uncertainty in the angular calculations has been estimated to be less than 0.1 degrees.

In Fig. 10, flight shortwave radiometer solar radiances which were reflected by the MAM's are presented. The radiance measurements exhibited the same trends with varying incident angle as was observed in the ground shortwave radiometer measurements. The flight and ground radiance profiles have the same FOV angular ranges. They both exhibited the same qualitative changes in intensity with the source off-axis angle. However, the dip which was observed in the NOAA-9 ground measurements was not found in the flight measurements. In Fig. 11, flight

shortwave solar radiances are presented which were measured using the total radiometers. The flight measurements exhibited a stronger variability with the off-axis incident angle than the ground measurements exhibited.

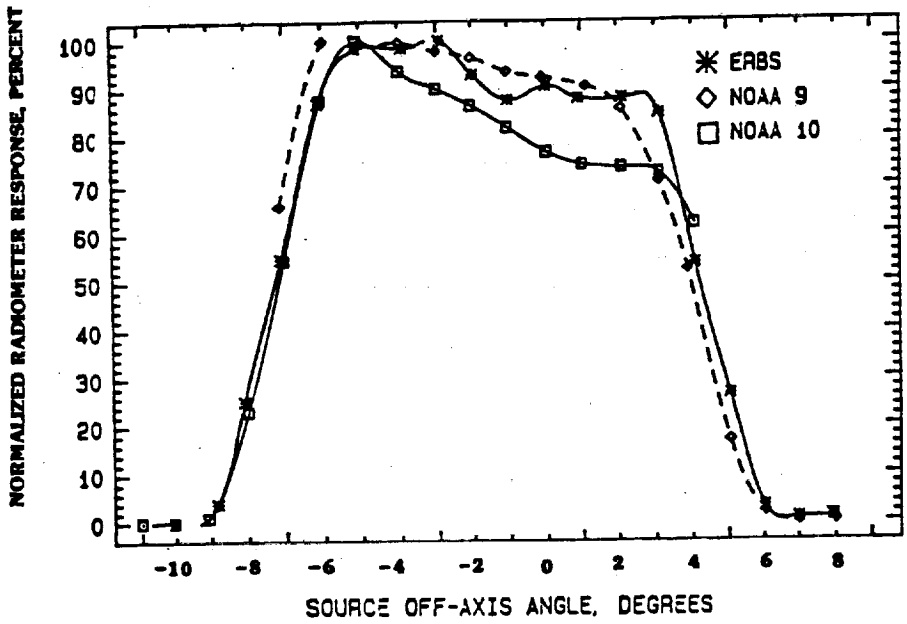

Fig. 10. Flight shortwave radiometer MAM-reflected solar radiances plotted as a function of angular distance of incident beam from the MAM baffle optical axis. In

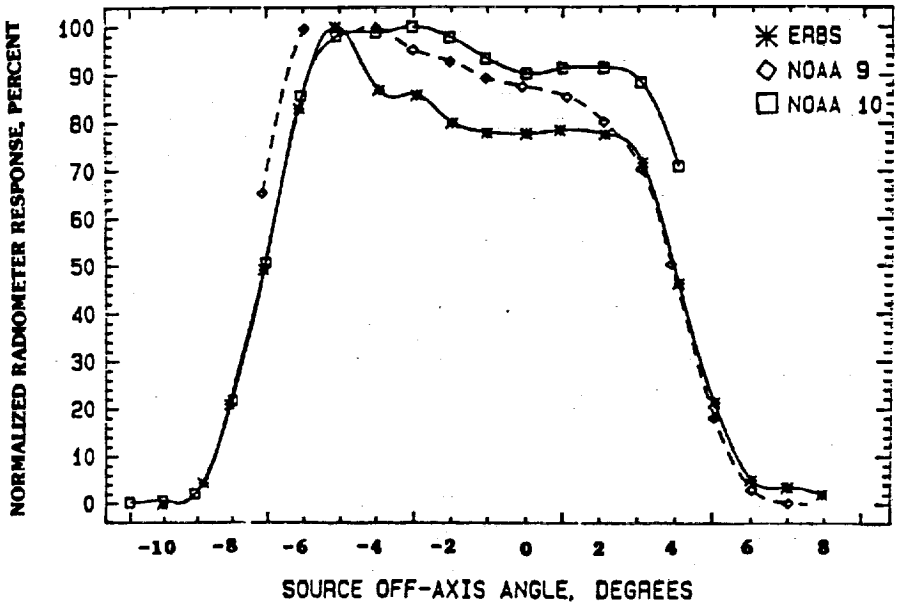

Fig. 11. Flight total radiometer MAM-reflected solar radiances plotted against angular distance of the incident beam from the optical axis of the MAM baffle.

In Fig. 12, ERBS solar calibration measurements are presented for the November 20, 1984, through October 16, 1985, period. The change in the reflected solar radiance

is presented as a function of time. The reflected solar radiance values were normalized to the mean Earth/Sun distance. The November 20, 1984 measurements provided the reference by which the changes in the gains of the shortwave and total radiometers were evaluated. For the total radiometer, changes are indicative of changes in the shortwave portion of the radiometer's gain and not changes in the longwave gain. The corrections for the emitted and reflected longwave components from the MAM were derived from least squares analyses of the total radiometer measurements of the MAM with no shortwave source present and the corresponding temperatures of the baffle and MAM mirror array. During the October 1984 through December 1989 period, the incident solar radiance, normalized to the mean Earth/Sun distance, was found to be essentially constant within 0.1%[14,15] using the ERBE solar monitors. The shortwave radiometer data set indicated that the shortwave gain was stable to within ±2% during the 11-month period. The scatter in the data was primarily caused by variability in the radiances as a function of incident angle, as was illustrated in Figs. 8 through 11. Most of the scatter in the Fig. 12 would not be present if the magnitude of the reflected radiances did not vary with incident angle.

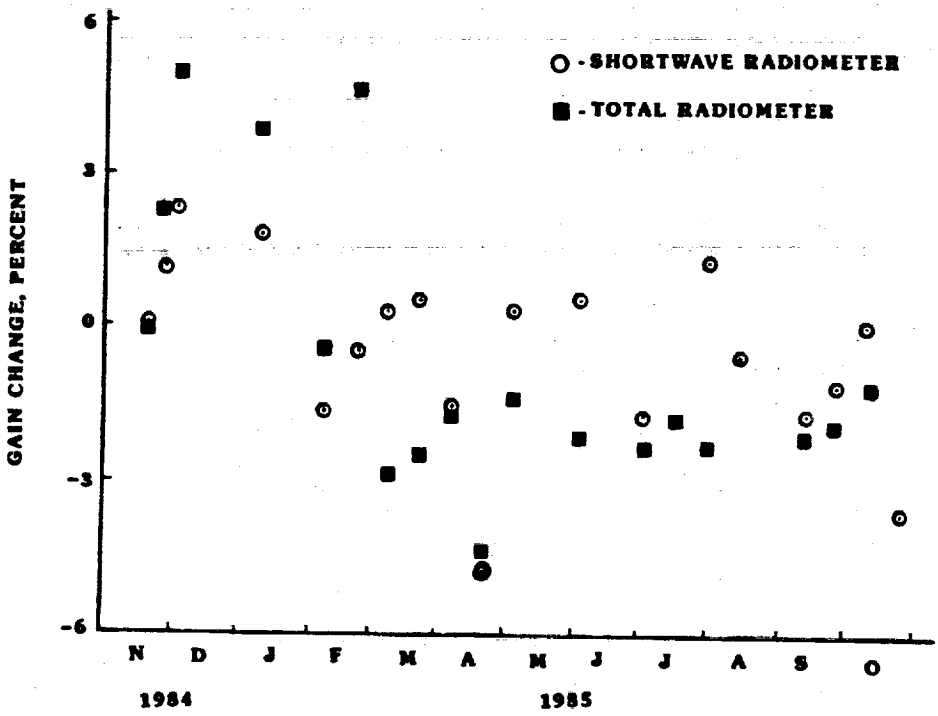

Fig. 12. ERBS solar calibrations time series.

The total radiometer data set suggests a decreasing trend. The data for the November 1984 through February 1985 period are approximately 7% higher than the data for the period after February 1985. The 7% difference represents a decrease in the sensitivity of the shortwave portion of the total radiometer. On February 28, 1985, the total and shortwave radiometers accidentally observed the Sun directly, at the space reference position, elevation angle of 14 degrees, for an extended period of time. The accident was caused by a temporary failure of the azimuthal position mechanism. The direct observations of the Sun caused decreases

in the shortwave portion of the total radiometer sensitivity. The longwave gain of the total radiometer did not change[9]. The shortwave radiometer did not experience any detectable changes in its sensitivity because its two Suprasil W1 filters protected the thermistor bolometer from direct exposure to the solar radiances.

In Fig. 13, the NOAA-9 flight solar calibration results are presented for the February 20, 1985, through December 24, 1986, period. The radiance measurements for February 20, 1985 were used as references in order to detect changes in the shortwave and total radiometers gains. The time series indicate that the radiances were stable to ±2%. The scatter is primarily caused by the variability of the radiance with off-axis incident angle. The ERBS and NOAA-9 measurements indicated that the reflective characteristics of the MAM assemblies did not degrade over exposure periods to space as much as 2 years.

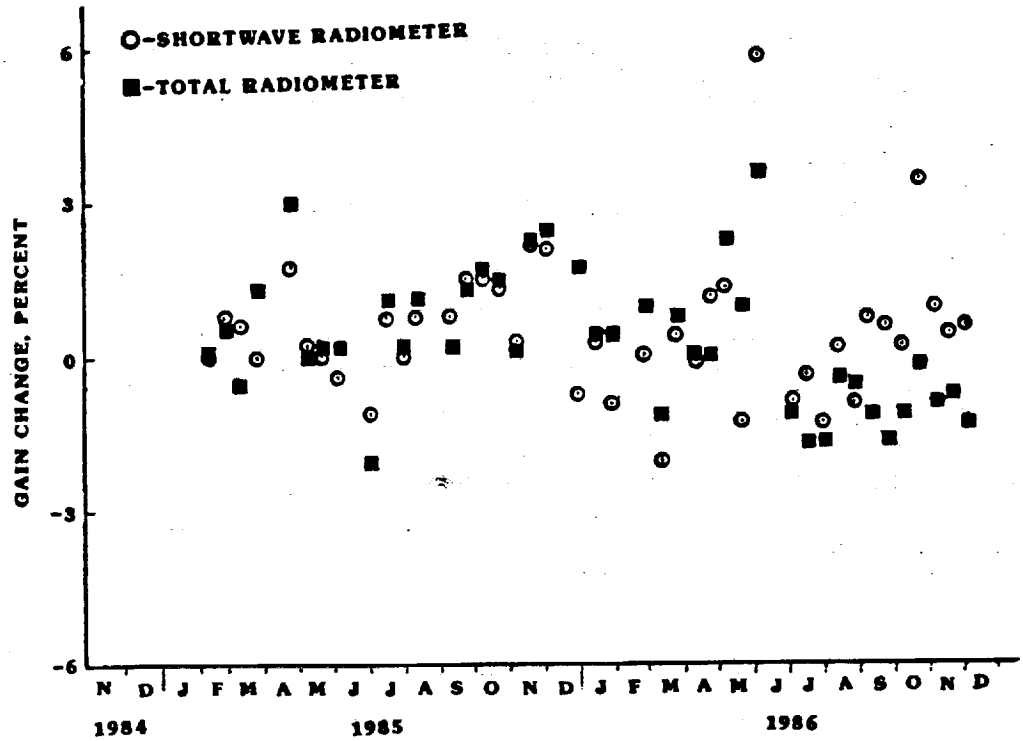

Fig. 13. NOAA-9 solar calibrations time series.

5. CONCLUSIONS

The MAM assemblies exhibited no detectable degradation in their reflectance properties over periods as much as 2 years. The flight solar calibration measurements indicate no significant changes above the 2% level in the amounts of solar radiances which were reflected by the MAM's of the shortwave radiometers. This result indicates that the reflectance properties of the MAM's did not degrade. In addition, this result suggests that the gains of the shortwave radiometers were stable at the ±2% level and that the Suprasil W1 filters did not exhibit any detectable degradation in their transmission properties. Suprasil W1 filters degrade very rapidly when exposed directly to solar ultraviolet radiation[8]. Since

the aluminum telescope mirrors and the MAM minimized the amounts of indirect ultraviolet radiation which were projected upon the filters, the filters should not have exhibited any significant degradation in their transmission properties. During February 1985, the sensitivity of the shortwave portion of the ERBS total radiometers decreased approximately 7% when the radiometers were exposed directly to the Sun. A correction for this 7% decrease has been incorporated in the ERBE data reduction algorithms.

6. REFERENCES

1. B. R. Barkstrom, E. F. Harrison, and R. B. Lee III, "Earth Radiation Budget Experiment/Preliminary Seasonal Results," Eos, vol. 71, no. 9, pp. 297-305, February 27, 1990.

2. V. Ramanathan, R. D. Cess, E. F. Harrison, P. Minis, B. R. Barkstrom, E. Ahmad, and D. Hartmann, "Cloud-Radiative Forcing and Climate: Results from the Earth Radiation Budget Experiment," Science, vol. 243, pp. 57-63, 1989.

3. B. R. Barkstrom, "The Earth Radiation Budget Experiment (ERBE)," Bull. Amer. Meteor. Soc., vol. 65, no. 11, pp. 1170-1185, 1984.

4. L. P. Kopia, "The Earth Radiation Budget Experiment Scanner Instrument," Rev. Geophys., vol. 24, no. 9, pp. 400-406, May 1986.

5. M. R. Luther, J. E. Cooper, and G. R. Taylor, "The Earth Radiation Budget Experiment Non-Scanning Instrument," Rev. Geophys., vol. 26, no. 2, pp. 391-399, May 1986.

6. R. B. Lee III, B. R. Barkstrom, and R. D. Cess, "Characteristics of the Earth Radiation Budget Experiment Solar Monitors," Appl. Opt., vol. 26, no. 15, pp. 3090-3096, 1987.

7. R. B. Lee III, M. A. Gibson, S. Thomas, J. R. Mahan, J. L. Meekins, and N. E. Tira, "Earth Radiation Budget Experiment Scanner Radiometric Calibration Results," SPIE Proc, vol. 1299, pp. 80-91, 1990.

8. J. Paden, R. S. Wilson, D. K. Pandey, S. Thomas, M. A. Gibson, and R. B. Lee III, "Ground and In-Flight Calibrations of the Earth Radiation Budget Experiment Non-Scanning Radiometers," SPIE Proc., vol. 1300, pp. 190-201, 1990.

9. R. B. Lee III, B. R. Barkstrom, N. Halyo, M. A. Gibson, and L. M. Avis, "Characterizations of the Earth Radiation Budget Experiment (ERBE) Scanning Radiometers," SPIE Proc., vol. 1109, pp. 186-194, 1989.

10. N. Halyo, D. K. Pandey, and D. B. Taylor, "Modeling and Characterization of the Earth Radiation Budget Experiment Nonscanner and Scanner Sensors," NASA Contractor Report 181818, March 1989.

11. R. Tousey, "Optical Problems of the Satellite," J. Opt. Soc. Am., vol. 47, no. 4, pp. 263, 1957.

12. G. Falbel and A. Iannararelli, "Radiometric Calibration for the Earth Radiation Budget Experiment Instruments," SPIE Proc., vol. 308, pp. 122-143, 1981.

13. L. P. Kopia and R. B. Lee III, "Earth Radiation Budget (ERBE) Scanner Instrument," SPIE Proc., vol. 1299, pp. 61-79, 1990.

14. R. B. Lee III, "Long-term Solar Irradiance Variability: 1984-1989 Observations," Proc. of Climate Impact of Solar Variability Conference, NASA Conference Publication 3086, NASA Goddard Space Flight Center, Greenbelt, Maryland, April 24-27, 1990.

15. R. B. Lee III, M. A. Woerner, M. A. Gibson, S. Thomas, and R. Wilson, "Total Solar Irradiance Variability: 5 Years of ERBE Data," Proc. Seventh Conference on Atmospheric Radiation, Amer. Meteorological Soc., Boston, Mass., pp. 126-129, July 23-27, 1990.